

Characteristics of bright ab-type RR Lyrae stars from the ASAS and WASP surveys

M. Skarka,^{1*}

¹*Department of Theoretical Physics and Astrophysics, Masaryk University, Kotlářská 2, 611 37 Brno, Czech Republic*

ABSTRACT

In this paper we present results based on high-density, high-precision WASP light curves supplemented with lower-precision photometry from ASAS for 268 RR Lyrae stars (176 regular, 92 Blazhko). Light curves were Fourier-decomposed, and coefficients from WASP were transformed to the ASAS standard using 24 common stars. Coefficients were then compared with similar data from Galactic globular clusters, the Galactic bulge, LMC, and SMC. Using Fourier coefficients we also calculated physical parameters via standard equations from the literature. We confirmed the results of previous authors, including lower amplitudes and longer rise times for Blazhko stars. It was found that in the R_{21} vs. $\log P$ plot the location of a star depends mainly on its metallicity and that Blazhko stars prefer a different location than modulation-free stars. Field and globular-cluster RR Lyrae variables have a different ϕ_{21} and ϕ_{31} than stars in the LMC, SMC and in Galactic bulge. Although there are some weak indications that Blazhko stars could prefer a slightly lower metallicity and shorter periods, no convincing proof was found. The most interesting highlight is the identification of a very recently proposed new group of metal-rich RR Lyrae type stars. These low-luminous, metal-strong variables, which comprise both Blazhko and regular stars, have shorter periods and about a 180 K higher temperature at constant $(B - V)_0$ than the rest of the stars in the sample.

Key words: methods: data analysis – techniques: photometric – stars: horizontal branch – stars: variables: RR Lyrae

1 INTRODUCTION

Recent research has revealed that the Blazhko effect (Blazhko 1907), which manifests itself as amplitude and/or phase changes in light curves of RR Lyrae type stars, is much more common than astronomers previously thought. Owing to ultra-precise space measurements provided by the *Kepler* and *CoRoT* satellites and extensive ground-based surveys (e.g. *The Konkoly Blazhko Survey*, Jurcsik et al. 2009a) it became apparent that the fraction of field RR Lyrae stars pulsating in fundamental mode, which undergo the Blazhko modulation, exceeds 50% (Jurcsik et al. 2009a; Benkő et al. 2010). Although these incidence rates are based on relatively small samples comprising only few tens of stars, the close to one half incidence of modulated stars could generally be correct.

In the first paper, which was devoted to bright RRab stars observed in the framework of the ASAS¹ (e.g. Pojmanski 1997, 2002) and WASP² (Pollacco et al. 2006; Butters et al. 2010) surveys, Skarka (2014) showed with a sample of more than three hundred stars that the incidence rate of bright field Blazhko RRab Lyraes is at least 31 %, which is much higher than previously presented by Szczygieł & Fabrycky (2007) (5.1 %, based on ASAS

data) or Wils et al. (2006), who proposed the fraction of Blazhko RR Lyrae stars based on NSVS (Woźniak et al. 2004) data as 4.1 %.

Concerning globular clusters, the situation is very similar. Jurcsik et al. (2012) found that one half of the RRab stars in M3 show modulation. In M5 the fraction of modulated stars is about 40 % (Jurcsik et al. 2011). Incidences of 20 %, 22 % and 30 % hold for the Large Magellanic Cloud (LMC, Soszyński et al. 2009), Small Magellanic Cloud (SMC, Soszyński et al. 2010) and galactic bulge (GB, Soszyński et al. 2011), respectively.

Evidently, understanding the Blazhko effect is of great importance. For the explanation of this phenomenon several models have been proposed. Among others we can mention *the magnetic model* (Shibahashi 2000), *resonance model* (Dziembowski & Mizerski 2004), *variable turbulent convection model* (Stothers 2006, 2010), which are more or less outdated, and new models, which were recently proposed: *shock wave model* (Gillet 2013), *starspot mechanism* (Stellingwerf et al. 2013) or *a hybrid model* (Bryant 2014). Nevertheless, the most commonly quoted model for explaining the Blazhko effect is *the radial resonance model* (Buchler & Kolláth 2011), which involves resonant interaction (9:2) between the fundamental and 9th overtone.

Except that it is unclear how the modulation should be modelled, there are two crucial questions unanswered: Why do some stars show modulation and other do not? Is there any difference

* maska@physics.muni.cz

¹ <http://www.astrouw.edu.pl/asas>

² <http://www.superwasp.org/>

between Blazhko and non-Blazhko stars? There are a few studies dealing mainly with the metallicity dependence of the Blazhko effect, such as the one by Moskalik & Poretti (2003), who suggested that the incidence rate of Blazhko stars could correlate with metallicity. However, a paper that broadly deals with other physical characteristics has been missing in spite of the availability of a large sample of regular and modulated field RRab stars.

Nevertheless, we should mention the study of Smolec (2005), who disproved the formerly noted suggestion of Moskalik & Poretti (2003) and gave plots for several interrelations among Fourier parameters of GB and LMC stars. Alcock et al. (2003) extensively compared stable and Blazhko stars (also in their Fourier parameters) in the LMC. More recently, Nemeč et al. (2011) gave a wide review of empirical relations which they applied to stars in the field of view of the *Kepler* space telescope and compared them with their spectroscopic results (Nemeč et al. 2013).

Jurcsik et al. (2011) showed that Blazhko RRab stars in M5 tend to have systematically larger amplitudes of light changes, shorter periods and fainter magnitudes than the averages of their sample stars. In addition they showed that Blazhko RRab Lyraes are bluer than regular stars and speculated that the Blazhko effect may have an evolutionary connection with the mode switch from fundamental to overtone-mode pulsation. Goranskij et al. (2010); Jurcsik et al. (2012) reported that V79 in M3 shares the properties of both the double-mode and the Blazhko phenomena. Similar behaviour was observed in OGLE-BLG-RRLYR-12245 (Soszyński et al. 2014). Jurcsik et al. (2013) found a very interesting stable star in the globular cluster M3, which mimics the behaviour of a Blazhko star. These objects could play an important role in understanding the nature of the Blazhko effect.

In this paper we concentrate on the analysis of Fourier parameters of stable and Blazhko field RRab stars brighter than 12.5 mag in maximum light with data from the WASP and ASAS surveys. In the second section information about data and methods of transformation of WASP parameters to those in the ASAS system are given. In addition data used from globular clusters and other stellar systems are discussed here. Section 3 presents methods used in the transformation of Fourier parameters to physical characteristics. In sec. 4 comparison of light-curve parameters of modulated and modulation-free stars (also for stars located in the LMC, SMC, GB and in globular clusters) are given. Section 5 provides a discussion on physical parameters. Finally, sec. 6 is a summary of this paper.

2 DATA SETS

The crucial part of our analysis, focused on stars from the Galactic field, is based on data from the WASP and ASAS databases. As an extension we also compiled and utilized available data of stars from globular clusters (hereafter GC), the LMC, SMC and GB and compared their light-curve parameters with those from our basic data set.

2.1 RR Lyrae sample from WASP and ASAS surveys

We examined the data of 321 RRab Lyraes from the ASAS and WASP surveys. These stars have well defined light curves brighter than 12.5 mag in maximum light. This analysis is a continuation of the study of Blazhko variables performed on the same sample (Skarka 2014). After additional visual examination, we discarded stars with sparse and uneven light curves and stars in which we

could not decide about modulation. That left us with 268 objects (176 stable stars, 92 Blazhko stars).

From this sample, 99 stars had high-density, high-precision data in the WASP survey containing typically few thousands of points per star, which span from several tens of days to about three years. Compared to ASAS light curves, which had typically only few hundreds of points spread out over several years, WASP data were of significantly better quality with a magnitude-order lower scatter than ASAS light curves. The reader is referred to Skarka (2014) for more details about the data, methods in data cleaning, data processing and period determination, as well as for methods to identify the Blazhko effect.

The goal of the light-curve analysis was to determine Fourier parameters $R_{i1} = A_i/A_1$ and $\phi_{i1} = \phi_i - i\phi_1$ via light-curve fitting with

$$m(t) = A_0 + \sum_{i=1}^n A_i \sin\left(2\pi i \frac{(t-t_0)}{P} + \phi_i\right), \quad (1)$$

where n is the degree of the fit, t_0 is a time of maximum light and P is the basic pulsation period. Fourier parameters, which were firstly introduced to analyse light-curve properties of Cepheids (Simon & Lee 1981), can be easily converted to physical characteristics through known empirical relations (sec. 3).

To be at least roughly objective, we applied a slightly modified approach introduced by Kovács (2005) (hereafter K05) for determination of the degree of fit for ASAS light curves. At first, a sixth order fit ($n = 6$ in eq. 1) was applied to each light curve. Subsequently, parameter m^* was calculated:

$$m^* = \text{ROUND} \left[\frac{A_1 \sqrt{n^*}}{20\sigma} \right]. \quad (2)$$

In the above equation A_1 is the first-component amplitude, σ is the uncertainty of the 6th order fit and n^* is the number of points in the particular light curve. Since we worked with about double the amount of data that K05 used, his constant 10 (in the denominator of eq. 2) was changed to 20 and his function INT was changed to ROUND. For $m^* < 4$ and $4 < m^* < 10$ a fit with $n = 4$ and $n = m^*$ components was used, respectively. If $m^* > 10$ than $n = 10$. Nevertheless, in several tens of stars, the degree of the fit was changed by visual inspection to get a better model of the light curve. Noted conditions were used to avoid over-fitting of noisy light curves and under-fitting of well defined ones as was already discussed in K05. In the case of WASP data, data were always fitted with ten components. Since WASP data were more dense and more numerous than those from ASAS, uncertainties of parameters based on WASP data were in the order of a few thousandths, while uncertainties of parameters derived from ASAS data were of a magnitude larger.

2.1.1 WASP and ASAS calibrations

The vast majority of relationships between Fourier parameters and physical characteristics (sec. 3) use Fourier coefficients based on V -light curve decomposition. ASAS measurements are in the V filter, and offsets of light-curve parameters from ASAS and those based on the standard V Johnson filter are known (table 3 in K05). Since we utilized only data from WASP and ASAS, the consistency between parameters from these two surveys was more important than precise calibration to the standard Johnsons V filter. Thus we decided to transform WASP broad-band light-curve parameters onto ASAS using 24 stars in common. Subsequently, values were shifted using Kovacs offsets.

When we compared WASP Fourier coefficients with those

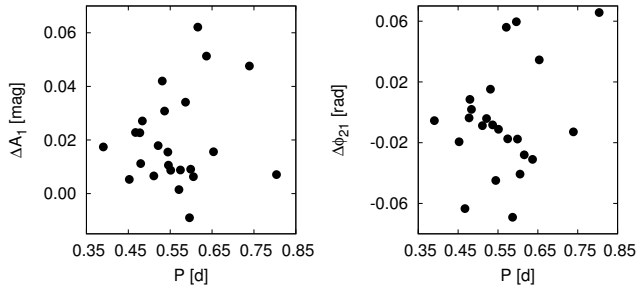


Figure 1. Offsets between WASP and ASAS in amplitude A_1 (left panel) and parameter ϕ_{21} (right panel).

from ASAS, it was found that offsets are very scattered (examples in fig. 1). Therefore, we considered a linear relation between WASP and ASAS parameters rather than simple shifts. The dependences were iteratively fitted using the weighted least-squares method, and outliers deviating more than 3σ were removed in each iteration. Resulting fits showing almost 1:1 relations are in fig. 2, and final parameters of the fits can be found in Table 1.

Despite the fact that the conversion from the WASP to ASAS system significantly increases the uncertainties, parameters based on WASP are given in the cases when the stars had both WASP and ASAS data available, because WASP light curves are much better defined. Derived Fourier parameters, converted to the standard system, together with physical characteristics and other properties of light curves, are given in sec. 3 in table 3.

2.2 Globular cluster RRab stars

Since many of RR Lyrae stars located in GC's have been studied in detail in the past two decades, a relatively large sample of their accurate Fourier coefficients is available. Unfortunately, in many of these RR Lyrae stars it is not possible to find information about their modulation, which reduces the number of suitable objects for our purpose.

Kovács & Walker (2001) compiled an extensive list of almost four hundred cluster RR Lyrae stars with Fourier decomposition. We scanned the literature (ω Cen (Jurcsik et al. 2001), M53 (Dékány & Kovács 2009; Arellano Ferro et al. 2011), M5 (Jurcsik et al. 2011), M3 (Jurcsik et al. 2012), M9 (Arellano Ferro et al. 2013), M62 (Contreras et al. 2010), NGC5466 (Arellano Ferro et al. 2008), NGC1851 (Walker 1998), NGC6171 (Clement & Shelton 1997), and IC4499 (Walker & Nemeč 1996)) to get information about the modulation of stars in the set of Kovács & Walker (2001), and to extend and enhance this list.

Contreras et al. (2010) provides only information about a deviation parameter D_m of stars in M62. This parameter was introduced by Jurcsik & Kovacs (1996) to give information about the quality and stability of the light curve. Usually, non-modulated stars are considered to have $D_m < 3$. Nevertheless, Cacciari et al. (2005) showed that D_m is effectively unable to distinguish between Blazko and non-Blazhko stars down to $D_m \leq 2$. Therefore, only stars in M62 with $D_m < 2$ were included in our list and were considered as stable stars. The final sample of GC RRab Lyraes that we used (Table 2, available as a supplement information at the CDS portal), contain 188 stars with stable light curves and 86 modulated stars.

Table 1. Parameters of the linear fit in the form $X_{ASAS} = a * X_{WASP} + b$. The third column with σ gives the standard deviation of the fit. The errors in the final digits of the corresponding parameter are given in parenthesis.

ID	a	b	σ
A_1	1.001(37)	0.015(13)	0.013
A_2	1.003(30)	0.005(5)	0.005
A_3	1.033(28)	0.001(3)	0.004
A_4	0.979(26)	0.004(2)	0.003
R_{21}	0.981(58)	0.004(28)	0.009
R_{31}	0.988(72)	0.002(24)	0.008
R_{41}	0.975(39)	0.003(8)	0.005
ϕ_{21}	0.960(31)	0.086(74)	0.016
ϕ_{31}	0.986(24)	0.052(118)	0.019
A_{tot}	1.027(33)	0.006(30)	0.034
RT	1.032(94)	0.005(15)	0.013

Table 2. Fourier parameters of Fundamental mode RR Lyrae variables located in globular clusters. The second column gives information about the modulation of the star. The complete table is only available at the CDS.

ID	BL	p [d]	A_1	R_{21}	R_{31}	ϕ_{21}	ϕ_{31}	ref.
M53 V1	-	0.6098	0.365	0.4904	0.3479	2.333	5.045	1
M3 V3	+	0.5582	0.408	0.4975	0.3358	2.307	4.968	2
...

When Fourier phase parameters from literature were based on cosine-term decomposition, they were transformed to sine-term using

$$\begin{aligned} \phi_{21}^s &= \phi_{21}^c - \pi/2 \\ \phi_{31}^s &= \phi_{31}^c + \pi. \end{aligned} \quad (3)$$

If necessary, ϕ_{21} and ϕ_{31} were corrected for integer multiples of π to meet $\phi_{21} < \pi$ and $\pi < \phi_{31} < 2\pi$ conditions.

2.3 Fourier parameters of RR Lyrae stars located in the LMC, SMC and GB

Fourier coefficients of RRab Lyraes observed in the framework of the OGLE-III survey (Udalski 2003; Udalski et al. 2008) were gathered through the WWW interface³ to have a comparison of field stars with stars in the GB (11 371 stars, Soszyński et al. 2011), LMC (16 941, Soszyński et al. 2009) and SMC (1 863, Soszyński et al. 2010). In the case of LMC stars we also used data of modulated stars (731 objects, Alcock et al. 2003).

Since Fourier decomposition of the OGLE data were available for the I passband and according to cosine-series, they were transformed to V filter to match our results using eq. 3 and relations introduced by Morgan et al. (1998).

3 PHYSICAL PARAMETERS DETERMINATION

As far back as the first pioneering studies of GCs in the first half of twentieth century, it became obvious that there is some correlation between period, metallicity, amplitude of light changes, and incidence rate of RRab and RRc stars in GCs (e.g. Oosterhoff 1939,

³ <http://ogledb.astrouw.edu.pl/~ogle/CVS/>

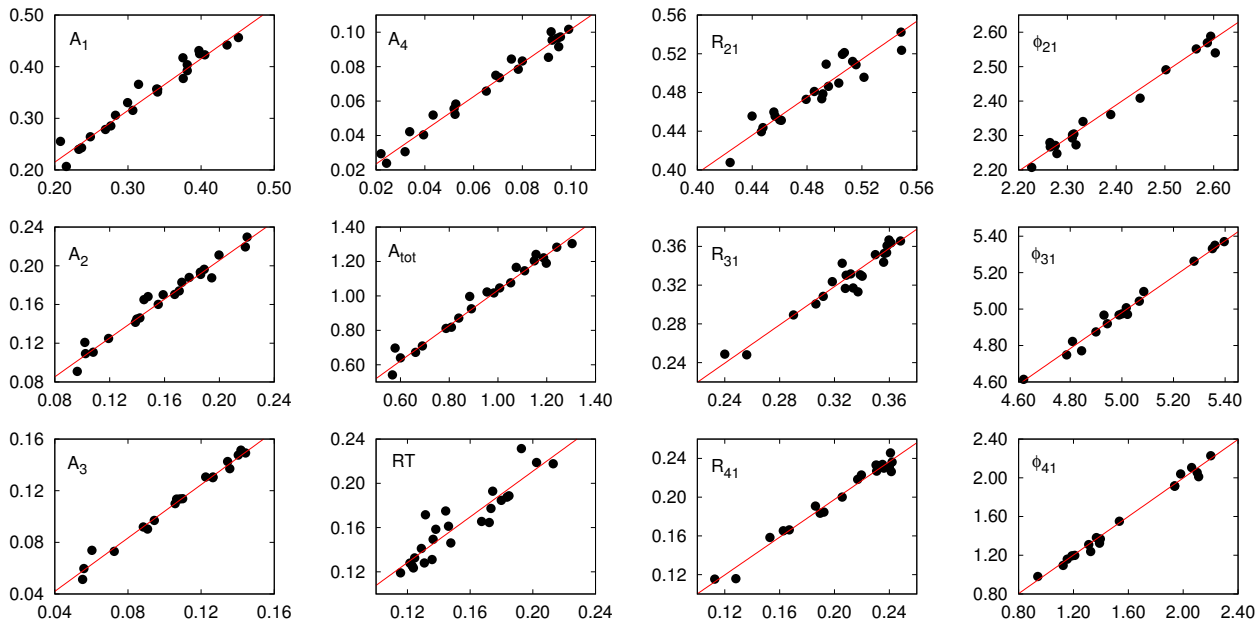


Figure 2. Weighted linear least square fits of various light-curve parameters. The WASP value is on the abscissa, while the ASAS value is on the ordinate. The corresponding parameter is labelled in the top left corner of each sub-plot. Outliers located more than 3σ from the fit were iteratively removed. Amplitudes are in magnitudes, ϕ_{i1} in radians and rise time (RT) in the part of the pulsation cycle. Parameters of each fit are in table 1.

1944; Arp 1955; Preston 1959). In particular, the average period of RRab stars in metal-deficient GCs was longer than in metal rich GCs and it seemed that RRab variables with lower metallicity tend to have lower amplitudes for a given period. This led to a definition of Oosterhoff groups. Sandage (1981) found that RRab members of GCs with a longer period at a given amplitude have a higher luminosity, which leads to a period-amplitude-luminosity relation. This was the first step towards physical parameters determination using light curve properties.

Later, it became apparent that not only the period and amplitude of the light changes, but that the shape of the light curve can tell us something about the physical parameters of RR Lyrae variables. After the introduction of Fourier parameters by Simon & Lee (1981) in cepheids, Simon & Teays (1982) showed the advantages in distinguishing between RRab and RRc stars using plots, where Fourier coefficients are plotted as a function of period.

The first studies on the relationships of Fourier coefficients and physical parameters of RR Lyrae stars were those of Simon (1985, 1988) and Simon & Clement (1993), who connected their results with theoretical models. These works were followed by papers of Kovacs & Zsoldos (1995) and Jurcsik & Kovacs (1996), who determined $[\text{Fe}/\text{H}] - P - \phi_{31}$ equations. Jurcsik (1998), Kovács & Walker (2001) and Sandage (2004) complemented and extended the package of empirical relations with equations for other physical parameters like absolute magnitude, temperature and others.

The applicability and correctness of these widely used calibrations were many times proved and discussed, and also modified. Therefore, it is sometimes difficult to be well informed. Examples of an extensive discussion on this topic can be found in papers of Cacciari et al. (2005) or Nemeč et al. (2011).

Fourier techniques can be used for stable stars, as well as for stars with the Blazhko effect that have uniformly and properly sampled light curves (see e.g. Kovács 2005; Smolec 2005; Jurcsik et al.

2009a)). In the case of modulated stars, Nemeč et al. (2013), who utilized new high-dispersion spectroscopic measurements and precise photometric data from the *Kepler* space telescope, recommend to determine $[\text{Fe}/\text{H}]$ as an average of metallicity during the Blazhko cycle, rather than to use a mean light-curve fit, which gives slightly inferior results.

Since we use ground-based data, which are often sparse (and therefore inappropriate for determination of parameters during modulation cycle), and with much poorer quality than data from space, our physical parameters are based on a mean-light-curve fit. In addition, the goal of this paper is to compare Blazhko stars with stable stars, not to precisely determine physical parameters. Therefore the use of a mean light curve should be of sufficient accuracy for our purpose.

3.1 Metallicity

For metallicity determination the calibration of Jurcsik & Kovacs (1996) was used

$$[\text{Fe}/\text{H}] = -5.038 - 5.394p + 1.345\phi_{31}. \quad (4)$$

This relation gives results, which are systematically larger by about 0.3 dex on the lowest metallicity limit, which was demonstrated on GCs (Jurcsik & Kovacs 1996; Nemeč 2004) and recently on field stars (Nemeč et al. 2013). Nevertheless, this discrepancy is not conspicuous in our $[\text{Fe}/\text{H}]_{\text{spec}}$ vs. $[\text{Fe}/\text{H}]_{\text{phot}}$ plot (fig. 3). Spectroscopic metallicity is taken from the Layden (1994) in Zinn & West (1984) scale (hereafter $[\text{Fe}/\text{H}]_{\text{ZW}}$). Photometric metallicity based on equation 4, which is on the Carretta & Gratton (1997) scale (hereafter $[\text{Fe}/\text{H}]_{\text{CG}}$), was transformed to $[\text{Fe}/\text{H}]_{\text{ZW}}$ via $[\text{Fe}/\text{H}]_{\text{ZW}} = 1.05[\text{Fe}/\text{H}]_{\text{CG}} - 0.20$ provided by (Sandage 2004).

From fig. 3 it is seen that our photometric metallicities agree very well with the spectroscopic ones. The solid line represents the line of equality, dotted lines above and below the diagonal line

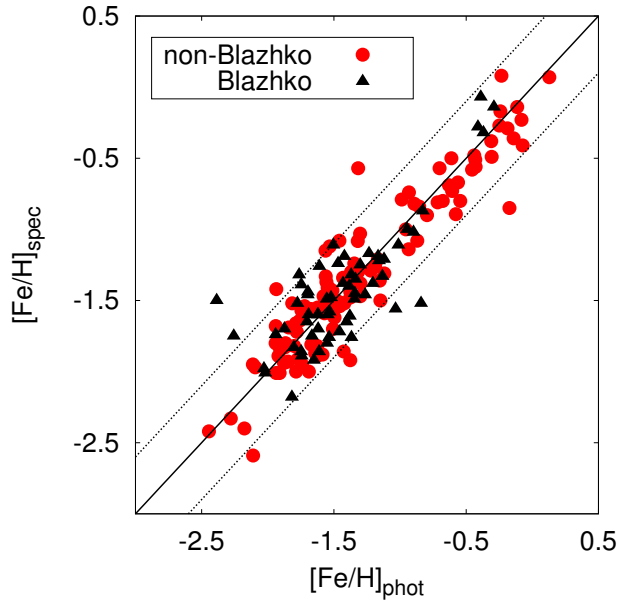


Figure 3. Spectroscopic (Layden 1994) versus photometric (this paper) metallicities on the ZW scale. The solid line is 1:1 relation, dotted lines denote 3σ limit. For details see the text.

show the 3σ limit of eq. 4 taken from Jurcsik & Kovacs (1996). Except for 13 outliers (5 Blazhko and 8 non-modulated stars), the remaining 161 stars are concentrated within this zone.

3.2 Other physical parameters

According to discussions in Nemeč et al. (2013) and Lee et al. (2014), we used a slightly modified relation of Jurcsik (1998) (her eq. 2) with the zero point decreased by a factor of 0.2 for absolute magnitude determination

$$M_V = 1.021 - 1.396p - 0.477A_1 + 0.103\phi_{31}. \quad (5)$$

Effective temperature was estimated using the following calibration of Kovács & Walker (2001):

$$\log T_{\text{eff}} = 3.884 + 0.3219(B-V)_0 + 0.0167 \log g + 0.007[\text{Fe}/\text{H}]_{\text{CG}}, \quad (6)$$

where $\log g = 2.473 - 1.226 \log p$. Extinction-free $(B-V)$

$$(B-V)_0 = 0.308 + 0.163p - 0.187A_1, \quad (7)$$

is from (Jurcsik 1998).

Finally, masses of stars were calculated through the calibration of Jurcsik (1998)

$$\log M = -0.328 - 0.062[\text{Fe}/\text{H}]_{\text{CG}}. \quad (8)$$

It is worth noting again that the goal of this study is a comparison between Blazhko and non-modulated stars, not precise determination of their parameters. In addition, comparison of different calibrations, which give slightly different results, and searching for the most reliable equations is out of scope of this paper. An extensive discussion and comparison of different calibrations can be found, for example, in Nemeč et al. (2011).

4 LIGHT-CURVE PROPERTIES OF REGULAR AND MODULATED RRAB STARS

In general, there are a few differences between Blazhko and non-Blazhko stars, which can be logically expected. As was noted by Szeidl (1988), who used a period-amplitude diagram (recently called the Bailey diagram), Blazhko stars gain a similar amplitude as modulation-free stars only during their maximum Blazhko phase. In other modulation phases their light changes are smaller. This means that the mean light curves of Blazhko stars have typically smaller amplitudes than stars with stable light changes.

As a direct consequence of lower amplitudes (at constant period), average light curves of modulated stars are more symmetrical than light curves of modulation-free stars. This further means a longer rise-time (RT , carrying information about a part of the cycle from minimum to maximum light) and lower amplitudes of higher components of Fourier fits for modulated stars, as already noted by Alcock et al. (2003) and Smolec (2005).

4.1 Amplitudes

Figure 4 shows the distribution of the observed total LC amplitude A_{tot} (difference between maximum and minimum light) and the first three Fourier amplitudes as a function of pulsation period of a star. Formerly noted facts are easily resolvable: Blazhko stars tend to have lower amplitudes than modulation-free stars. There is no distinct difference in the first Fourier amplitude A_1 (average values 0.342(6) and 0.331(7) for modulation-free and Blazhko stars, respectively), while higher-order amplitudes differ significantly ($A_{2,\text{Ave}} = 0.171(3)$ and $A_{3,\text{Ave}} = 0.113(3)$ for non-modulated stars and $A_{2,\text{Ave}} = 0.148(4)$ and $A_{3,\text{Ave}} = 0.088(3)$ for Blazhko stars). This means that the reduction in total amplitudes of modulated stars is caused by higher-order Fourier amplitudes. From Table 4, it is apparent that the trend of lower amplitudes for modulated stars is period-independent. For comparison, there are also GC stars plotted in fig. 4 (empty symbols). No apparent difference between GC and field stars was found.

The top left panel of fig. 4 shows a classical Bailey diagram, which is usually used for distinguishing between RR Lyrae types, as well as for investigation of membership to any of the Oosterhoff groups (Oosterhoff 1939, 1944). Recent studies have revealed that the correlation between Oosterhoff groups, metallicity and amplitudes of their RR Lyrae members is not as simple as it appears, and that there are probably more than two Oosterhoff groups (see, for example, reviews of Catelan 2009; Smith et al. 2011). Except for sec. 5.4, we do not deal with the Oosterhoff phenomenon, because our sample is very limited and spread over the whole sky. For those who are interested in this topic, we refer to the studies of Szczygieł et al. (2009) and Kinemuchi et al. (2006), which were based on much wider samples of stars observed in the ASAS and NSVS surveys.

Nevertheless, it is worth mentioning that Blazhko stars probably do not prefer any of the Oosterhoff groups, as it is apparent from the top left panel of fig. 4 where the two dotted lines illustrate empirical loci of Oosterhoff groups according to Szczygieł et al. (2009). From the same part of fig. 4, it is obvious that Blazhko stars have smaller total mean amplitudes ($A_{\text{totBL}} = 0.89 \pm 0.02$ mag) than their regular counterparts ($A_{\text{totSTABIL}} = 1.01 \pm 0.02$ mag).

If A_2 and A_3 are plotted as a function of A_1 we obtain the plots showed in the top panels of fig. 5. Again, Blazhko stars tend to have lower Fourier amplitudes. Below the limit of $A_1 \sim 0.2$ it seems, that modulated stars follow the trend of stable stars fairly well. Similar

Table 3. Parameters of sample stars. In the second column ‘a’ and ‘w’ means that parameters are based on ASAS and WASP data, respectively. The last column gives information about modulation. The errors in the final digits of the corresponding parameter are given in parenthesis. The full table is available electronically at the CDS.

ID	n	p [d]	A_1 [mag]	R_{21}	R_{31}	ϕ_{21} [rad]	ϕ_{31} [rad]	A_{tot} [mag]	RT [phase]	$[Fe/H]_{CG}$	M_V [mag]	T_{ef} [K]	$(B-V)_0$	\mathcal{M} [M_{\odot}]	BL
SW And	w	0.4422605(8)	0.3212(3)	0.545(1)	0.325(1)	2.615(3)	5.441(4)	0.94	0.18	-0.11(4)	0.81(11)	6745(18)	0.320(3)	0.48(2)	-
...

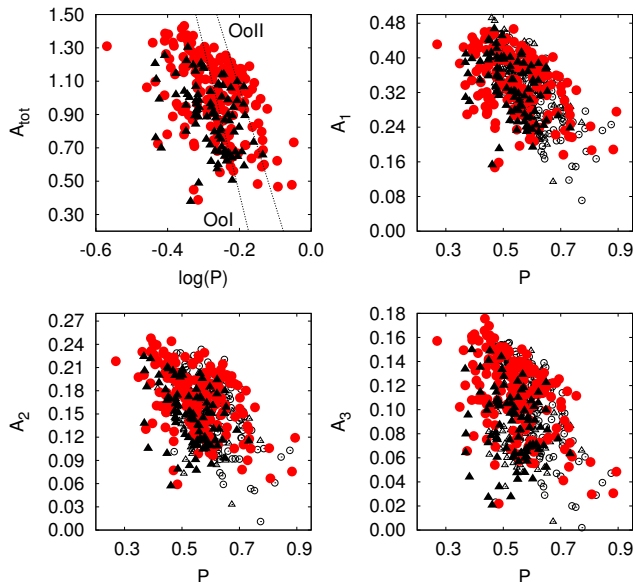


Figure 4. Period-amplitude diagrams for field RR Lyrae stars (filled symbols) and their counterparts in GCs (open symbols). Blazhko stars are depicted as triangles, while stable stars are plotted with circles. Pulsation period on the abscissa is in days, while amplitudes are in magnitudes.

Table 4. Average amplitudes for different period intervals. Values in parentheses are standard errors of the means. ‘S’ means stable stars and ‘BL’ modulated stars, respectively.

	$p \leq 0.5$		$p \in (0.5, 0.6)$		$p \geq 0.6$	
	S	BL	S	BL	S	BL
A_1	0.370(9)	0.369(12)	0.342(8)	0.316(9)	0.306(10)	0.294(15)
A_2	0.192(5)	0.167(7)	0.166(4)	0.139(6)	0.150(6)	0.135(8)
A_3	0.127(4)	0.095(6)	0.113(4)	0.084(4)	0.096(5)	0.082(6)

behaviour was noticed in GB stars by Smolec (2005) for I -band light curves. However, this statement is based only on three modulated field stars and two GC stars. In the bottom panel A_1 is plotted against the total amplitude A_{tot} of a star. A fleeting glance indicates that Blazhko stars are well separated from regular stars, which is not surprising, because A_1 is the dominant component of the total amplitude of Blazhko stars. With the unprecedented precise measurements of the *Kepler* satellite, Nemeč et al. (2011) found this dependence likely to be cubic.

From fig. 4 it is also apparent that the range of possible amplitudes decreases when the period increases for both Blazhko and non-modulated stars. Nevertheless, this does not mean that stars with a longer period automatically have a smaller amplitude (see fig. 2 and discussion in Nemeč et al. 2011).

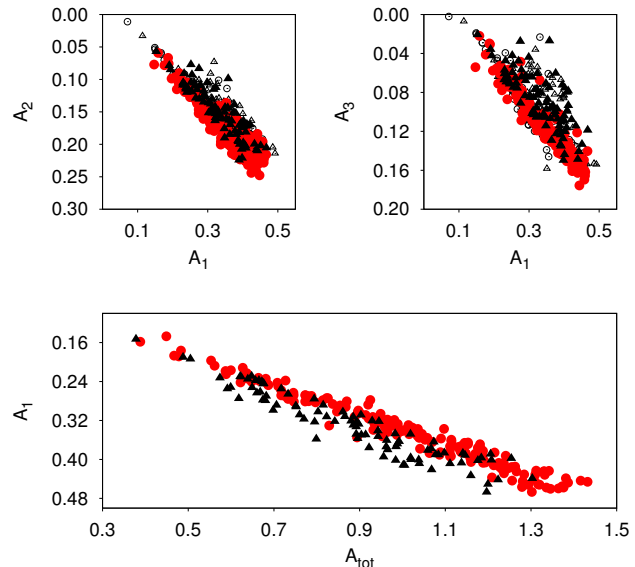


Figure 5. Correlations between Fourier amplitudes (in magnitudes). The top panels show dependencies of higher-order amplitudes on A_1 , while A_1 is plotted against the total amplitude of light changes in the bottom panel. Symbols are the same as in fig. 4.

4.2 Fourier parameters R_{21} and R_{31}

All differences in Fourier amplitudes get more evident when R_{31} is plotted as a function of R_{21} (fig. 6). In this figure, the dependence has the shape of a bent pin, where stars accumulate along the diagonal stem and around the horizontal pinhead. For comparison, modulation-free RR Lyrae stars from the LMC, SMC, and GB are plotted in this figure.

Evidently, Blazhko stars are located along the stem and regular stars prefer the pinhead around $\bar{R}_{31} \approx 0.34$ (average of all stable stars is 0.326(3)). This is also apparent from the right-hand panel of fig. 7, where the distribution of stars according to their R_{21} and \bar{R}_{31} are plotted. Below $\bar{R}_{31} = 0.3$ about 69% of the stars are Blazhko stars. Similarly for $\bar{R}_{31} < 0.25$ only 6% of the stars are stable stars. These 11 outlier-stars are labelled in fig. 6. Either they are long period RR Lyrae stars ($p > 0.7$ d), or are somehow peculiar. AL CMi⁴, RW TrA and FW Lup have unusually high photometric metallicity exceeding $[Fe/H]_{ZW} = 0.0$, or even higher. However, this would probably not be the cause of their location, because there are also GC stars with a variety of metallicities located in this region. MS Ara, AL CMi and V556 Hya show some scatter in their light curves, but they are considered as stars with stable light variations. The bottom-left detail (a) in fig. 6 depicts stable stars with

⁴ AL CMi has a spectroscopic metallicity much lower than photometric ($[Fe/H]_{ZW} = -0.81$, Layden 1994).

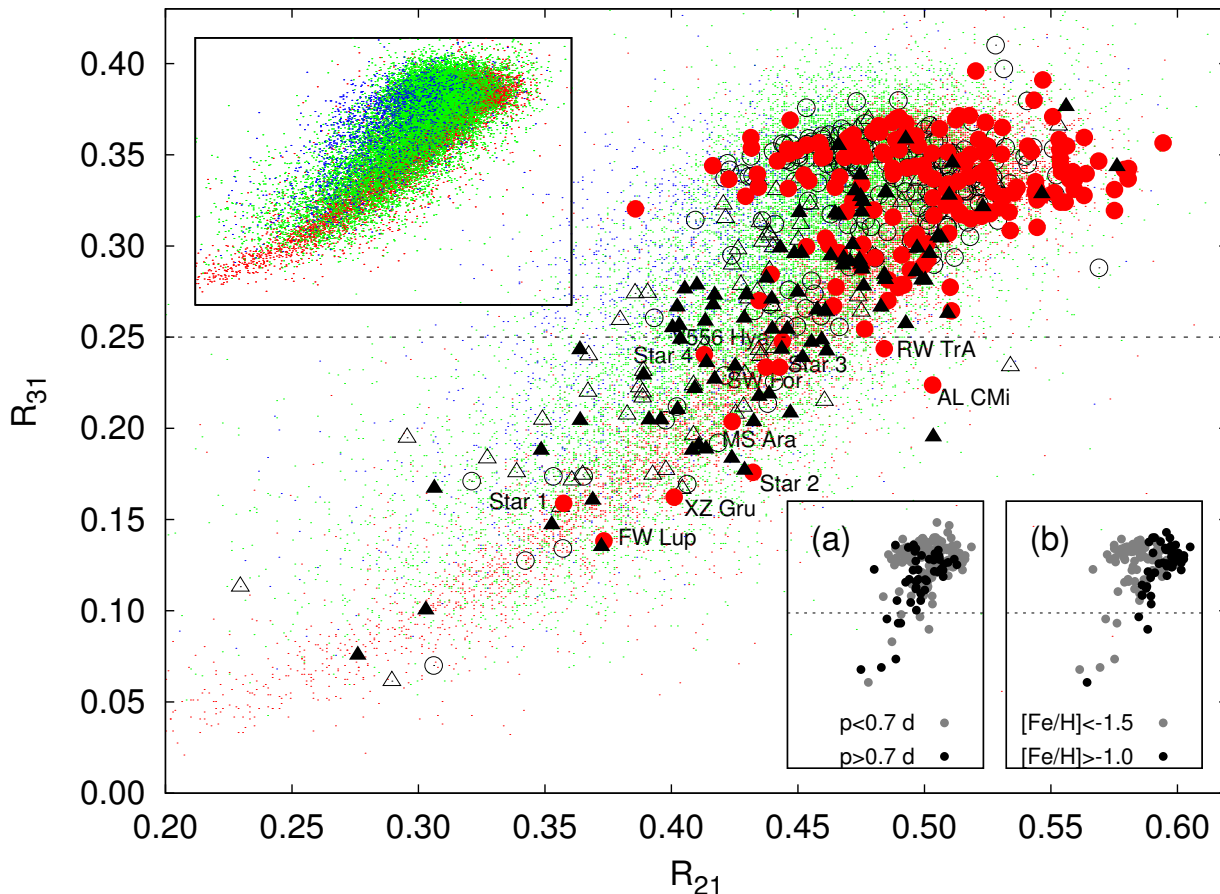


Figure 6. The correlation between R_{31} and R_{21} . In the main plot, as well as in the top-left detail, there are LMC (green dots), SMC (blue dots) and GB (red dots) plotted together with field and GC stars (the same symbols as in fig. 4, for better arrangement see the electronic version of the article). The dotted line represents 0.25-limit, below which Blazhko stars constitute the majority of the RRAb population. For information about labelled stars see the text. Star 1 corresponds to ASAS 134046+1749.2, Star 2 is ASAS083412-6836.1, Star 3 is ASAS 165126-2434.9 and Star 4 corresponds to ASAS160332-7053.4. In the bottom-right panel (a), modulation-free stars are distinguished with respect to their periods. Panel (b) shows regular stars drawn with different symbols for different metallicity. The same scale is used for all the plots.

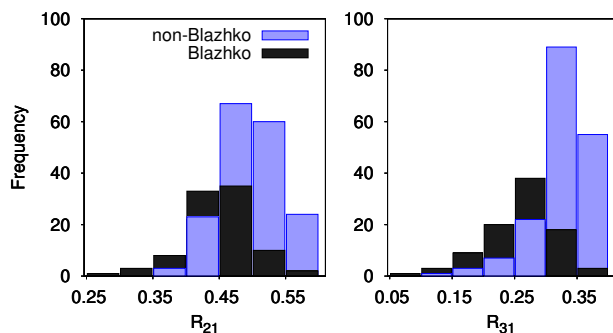


Figure 7. The distribution of Fourier amplitudes R_{21} and R_{31} for the studied stars. In the left-hand panel a significant drop in the stable-star population is apparent below $R_{31} \approx 0.3$.

respect to their periods. It is clear that the long-period variables prefer the diagonal stem rather than the pinhead.

The top left close-up of fig. 6 shows only data for the GB, LMC and SMC for better arrangement. When looking carefully, it is apparent that the dependences are slightly different and shifted. LMC (green dots) and SMC points (blue dots) are more scattered and shifted to the left, while data of stars located in the GB (red dots) are sharply defined on the right edge of the plot. It is very probable that this feature correlates mainly with metallicity. Stars with higher metallicity tend to be more to the right in this plot. SMC stars with the lowest average metallicity of about $[\text{Fe}/\text{H}]_{\text{ZW}} \approx -1.72$ (Kapakos & Hatzidimitriou 2012) are mostly to the left, LMC RR Lyrae stars with $[\text{Fe}/\text{H}]_{\text{ZW}} \approx -1.48$ in the middle, and GB stars with $[\text{Fe}/\text{H}]_{\text{ZW}} \approx -1.23$ (both from Smolec 2005) are mostly to the right.

The metallicity assumption is supported by the appearance of the bottom-right (b) panel of fig. 6, and also by theoretical models. Nemeč et al. (2011) presented predicted Fourier parameters calculated with the Warsaw convective-pulsation codes (Smolec & Moskalik 2008). Since they studied stars observed by the *Kepler* satellite, they obtained a similar dependence as in the upper part of fig. 6. Nevertheless, the situation is not simply just

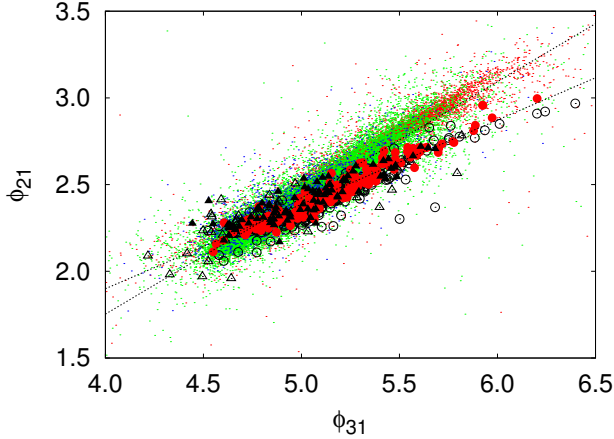


Figure 8. Fourier phase ϕ_{21} as a function of ϕ_{31} . Symbols are as in fig. 6. The dotted lines highlight the different inclination of the dependence for field and GC RR Lyrae stars, and for LMC, SMC and GB stars is easily noticeable.

metallicity-dependent, because the position in the ϕ_{31} versus R_{21} plot depends also mainly on the luminosity and mass of a star (see fig. 14 and 15 of Nemeč et al. 2011).

4.3 Fourier phases ϕ_{21} and ϕ_{31}

In fig. 8 it can be seen that the relationship between ϕ_{21} and ϕ_{31} is nearly linear, which was also observed in the *Kepler*-field stars, but this dependence was not so pronounced in synthetic diagrams (Nemeč et al. 2011). Noted discrepancies between observation and theory need to be investigated more closely.

From fig. 8 it is evident that the slope of field and GC stars is different than the slope of the dependence for stars from the LMC, SMC and GB (both dependences are highlighted by dotted lines, which are based on linear fits). The reason for this property is apparent in the details of fig. 9. Since the dependences of ϕ_{21} and ϕ_{31} for field and GC stars are linear and parallel in the whole range of periods, the vast majority of stars in the LMC and GB stars follow the dependence, which curves to higher values at the point of about $P = 0.55$ d. The reason for this phenomenon is not clear. Evolutionary effects are suspected to be responsible for this interesting behaviour. As a consequence, linear $P - [\text{Fe}/\text{H}] - \phi_{31}$ calibrations based on field and GC stars would very likely give incorrect results for LMC, SMC and GB RR Lyrae stars.

The bottom panel of fig. 9 shows the traditional result that at a constant period more metal-abundant stars have a higher ϕ_{31} , which is consistent with theoretical predictions when keeping mass and luminosity constant (see the bottom left panel of fig. 15 in Nemeč et al. 2011). Nemeč et al. (2011) also suggested that the lowest- L stars are expected to have a low ϕ_{21} , and that Blazhko stars should prefer a higher metallicity (due to a lower A_{tot} and higher ϕ_{31}). Our results contradict this statement, because many of the low-luminous RR Lyrae stars have a high ϕ_{21} , and Blazhko stars have on average a lower ϕ_{31} than regular RR Lyrae stars. This indicates that results on several RRab stars in the *Kepler* field can not be extrapolated to the wider sample. Low-luminous stars form a separated sequence in ϕ_{21} and ϕ_{31} vs. P diagrams ($\phi_{21} \geq 2.5$, $\phi_{31} \geq 5$ and $P < 0.6$ d), and correspond to metal-strong Oosterhoff I stars (see sec. 5.4).

Table 5. Average ϕ_{21} , ϕ_{31} and RT values for different period ranges. Numbers in parentheses are the standard errors of the means. ‘S’ denotes stable stars and ‘BL’ modulated stars, respectively.

	$p \leq 0.5$		$p \in (0.5, 0.6)$		$p \geq 0.6$	
	S	BL	S	BL	S	BL
ϕ_{21}	2.41(2)	2.37(3)	2.41(2)	2.43(2)	2.55(3)	2.49(3)
ϕ_{31}	5.08(4)	4.93(5)	5.08(4)	5.03(4)	5.32(5)	5.22(6)
RT	0.152(4)	0.225(12)	0.159(4)	0.227(12)	0.176(5)	0.200(8)

The differences in their average values of ϕ_{21} and ϕ_{31} for modulated and non-modulated stars over the same period interval are very small. We obtain $\phi_{21\text{ave}} = 2.45(2)$ and $\phi_{21\text{ave}} = 2.42(2)$ for stable and modulated stars over the whole period interval, respectively. The situation is similar for ϕ_{31} , where regular RR Lyrae stars have $\phi_{31\text{avg}} = 5.14(3)$, while modulated stars have $\phi_{31\text{avg}} = 5.03(2)$. From Table 5 we see that between the periods 0.5 and 0.6 days the averages of ϕ_{21} and ϕ_{31} are almost the same. Over other period ranges the differences are slightly more pronounced.

4.4 Rise time

Figure 10 shows how rise time correlates with some light-curve characteristics. It is seen that stable stars follow roughly linear trends, while RT s of modulated stars are very scattered and with typically higher values than for non-modulated stars. From these plots RT appears to be a powerful indicator predicting which stars are Blazhko-modulated. It appears that 1/3 of stars ($RT > 0.24$) can be clearly separated from stable stars. If an RRab star with $RT > 0.24$ is found, the star can be predicted to be a Blazhko star with pretty high confidence.

When looking carefully, the top left panel of fig. 10 is, after reversing the vertical axis, very similar to dependencies in fig. 9 for stable stars. This means that RT can also be used for metallicity determination (Sandage 2004). Nevertheless, the RT -metallicity equation can be used only for modulation-free stars, because Blazhko stars do not behave linearly and results for these stars would be completely wrong or at least systematically shifted.

In Table 5, it can be found how average RT behaves in different period ranges. As can be expected, a longer period means a higher rise time. For stars with regular light curves, the average rise time is $RT_{\text{ave}} = 0.161(3)$ over the whole period interval, while for modulated stars it is $RT_{\text{ave}} = 0.221(7)$.

5 DISCUSSION ON PHYSICAL PARAMETERS

In our analysis we assume that equations 4-8 work for both stable and Blazhko stars. This implies that different coefficients for modulated RR Lyrae stars would result in different physical parameters. However, we can not rule out the possibility that slightly different or additional physics occurs inside Blazhko stars. In such case, although Blazhko and stable stars would share the same physical parameters, their light-curve parameters would be different. Since at this moment no signs of different physics are apparent, we assume that different light-curve parameters mean different physical parameters.

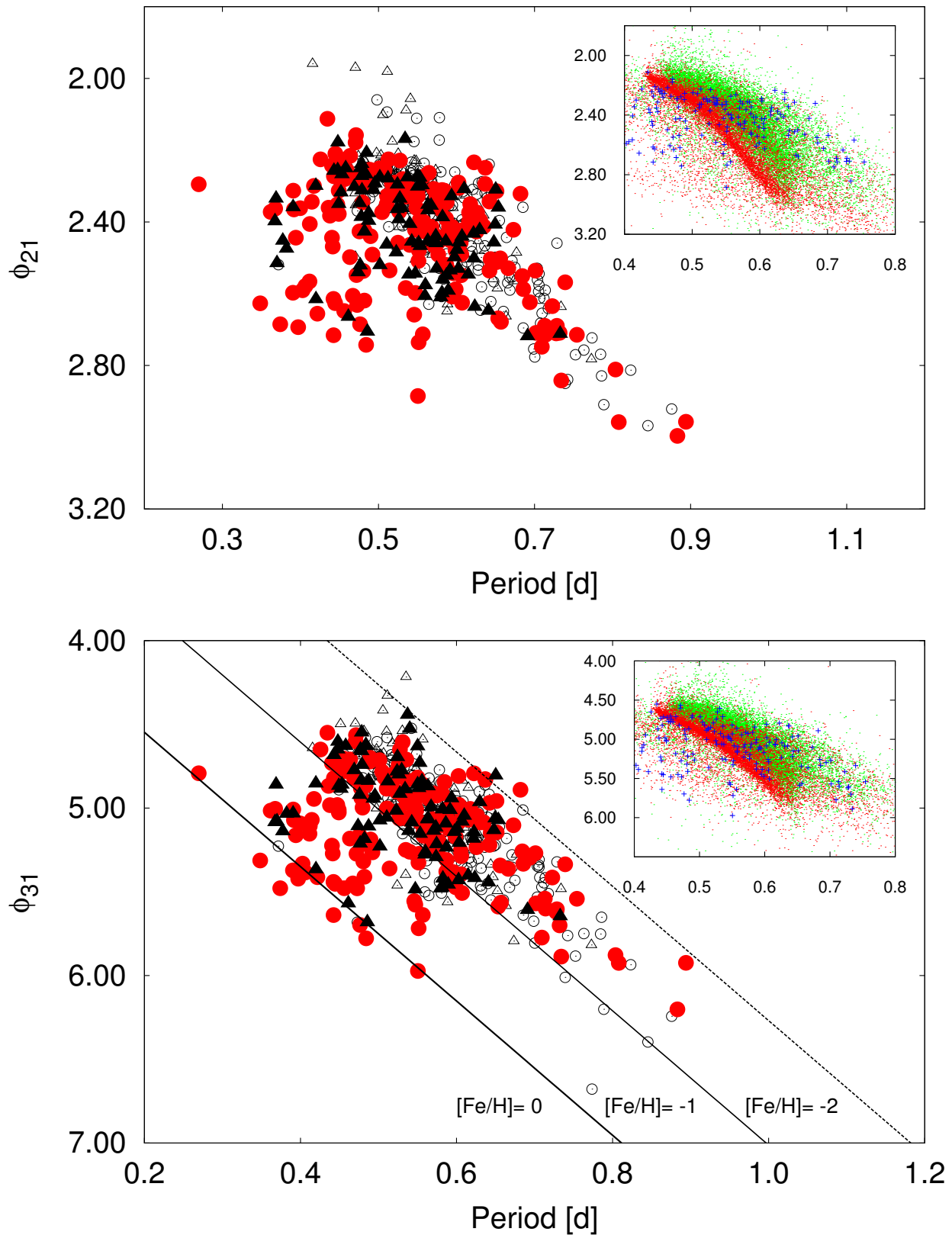


Figure 9. Distribution of Fourier phases according to period (in days) of a star. Symbols are the same as in fig. 3. For comparison, there are stable field stars (blue crosses), LMC (green dots) and GB stars (red dots) in the details of each plot. For a better representation see the online version. The lines in the bottom panel show points with the same metallicity ($[\text{Fe}/\text{H}]_{\text{CG}} = 0; -1; \text{ and } -2$ according to eq. 4).

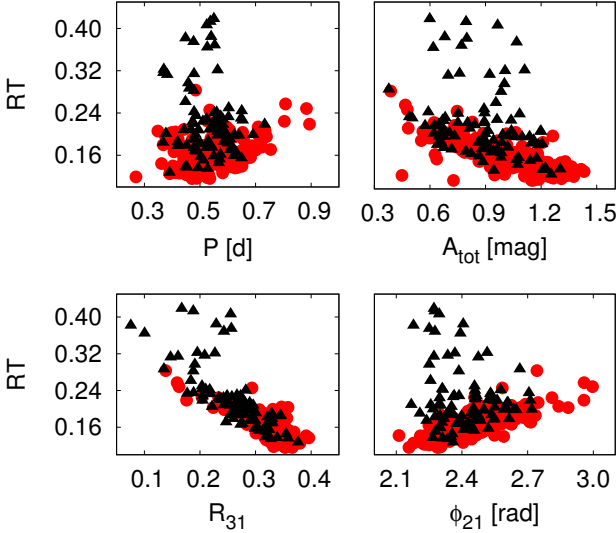


Figure 10. Rise time as a function of various light-curve parameters. Non-modulated stars are, as in other figures, plotted with red circles, modulated stars are drawn with black triangles.

5.1 Remarks on period distribution

The period-range of our 268 sample stars is between 0.27 and 0.89 days, which is also the range for our regular RR Lyrae stars. Periods of modulated stars range from 0.36 to 0.73 days. To test if the two samples come from the same distribution the Kolmogorov-Smirnov test was performed. The p-value 0.321 implies that they are consistent. The largest difference between the distributions (shown in the bottom panel of fig. 11) is at $P = 0.65$ d and exceeds $D = 0.121$. The appearance of the cumulative plot together with the histogram in fig. 11 point out the weak lack of Blazhko stars in the long-period part of the distribution.

Jursik et al. (2011) found that Blazhko stars in GC M5 have a preference for shorter periods (0.504 d) compared with the mean period of all RRAb stars (0.546 d). They proposed the occurrence rate of modulated stars in M5 with period shorter than 0.55 d as about 60%. In our sample, the percentage of Blazhko stars below and above this limit is almost identical (34.8% and 33.9%, respectively). Concerning periods, the mean period of all sample RRAb stars is 0.542(6) d, while the average period of Blazhko stars is only slightly lower (within the errors equal to 0.532(8) d). Modulated stars in the LMC have an average period of 0.552 d (Alcock et al. 2003), whereas all RRAb stars have an average period of 0.573 d. Although the tendency of modulated stars to have shorter periods is obvious for M5 and the LMC, the difference for field stars is not conclusive. To solve this problem, a more numerous sample would be needed. In addition the reanalysis of LMC stars (comprising new measurements since 2003) could shed some light on this matter.

5.2 Metallicity of non-modulated and Blazhko stars

When thinking about differences between modulated and modulation-free stars, metallicity is one of the most suspect parameters. Moskalik & Poretti (2003) assumed modulated stars in the GB to show a preference for higher metallicity, which was later disproved by Smolec (2005), who found that the occur-

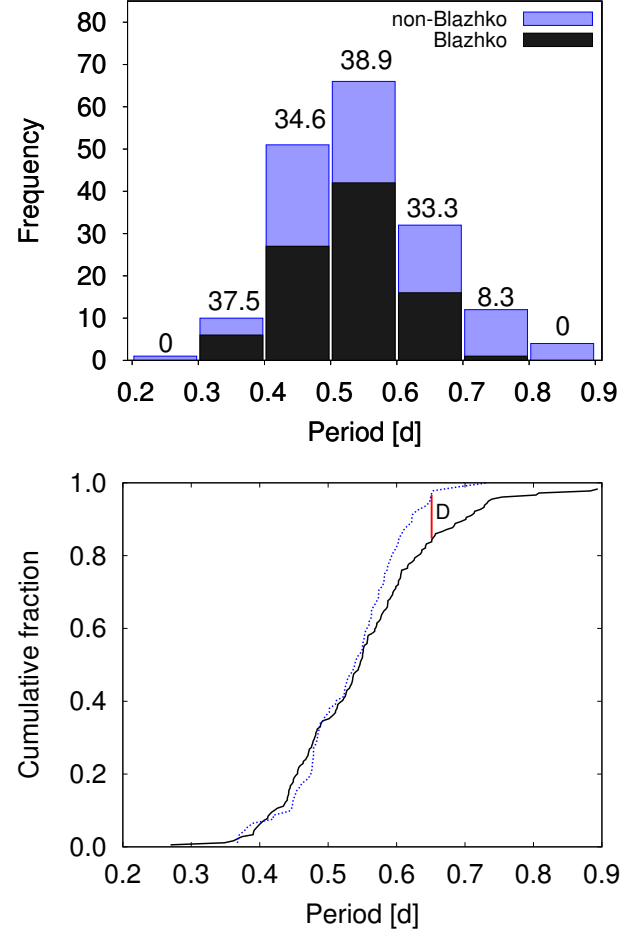


Figure 11. Distribution of sample stars according to their period (top panel) and their cumulative plots (bottom panel, the continuous black line is for regular stars, dotted for modulated stars). Numbers above each bin in the top panel give information about the percentage of Blazhko stars in each bin. Parameter D in the bottom panel shows the largest difference between the two populations.

rence of Blazhko stars is metallicity-independent. Although the Kolmogorov-Smirnov test showed the Blazhko sample to be consistent with the regular-stars sample ($p = 0.333$, $D = 0.120$ at $[\text{Fe}/\text{H}]_{\text{ZW}} = -0.94$), from the cumulative distribution function and histogram in fig. 12, it seems that Blazhko stars could subtly prefer lower metallicity. The incidence rate of Blazhko stars with $[\text{Fe}/\text{H}]_{\text{ZW}} < -1$ is about 38%, while among stars with $[\text{Fe}/\text{H}]_{\text{ZW}} > -1$ it is only 23%. Average values of metallicity are $[\text{Fe}/\text{H}]_{\text{ZW,avg}} = -1.40(5)$ for modulated stars, and $[\text{Fe}/\text{H}]_{\text{ZW,avg}} = -1.32(5)$ for variables with a stable light curve, respectively. These numbers are similar and can be considered as equal according to their errors.

Nevertheless, these statistics can be affected by selection effects. It is probable that some metal-rich modulated stars could remain undisclosed, because of the possible small modulation amplitude of these stars. For example, DM Cyg, SS Cnc and RS Boo (all with $[\text{Fe}/\text{H}]_{\text{ZW}} > -0.5$, Layden 1994) have modulation amplitudes of only about 0.1 mag. As in the case of basic pulsation periods, our analysis can not conclusively confirm metallicity dependence as an indicator of the occurrence rate of Blazhko stars. No metallicity dependence of the modulation period was noticed.

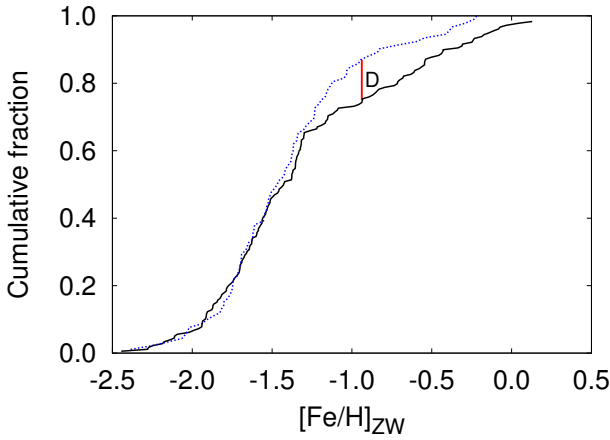
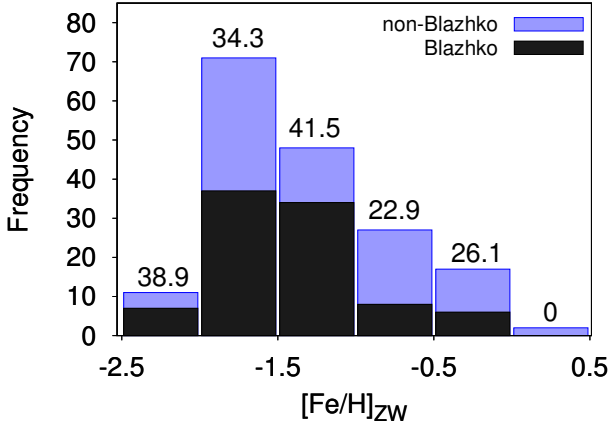


Figure 12. Distribution of sample stars according to their metallicity (top panel) and their cumulative plot (bottom panel, the black solid line is for regular stars, dotted for modulated stars). Numbers above each bin in the top panel and parameter D in the bottom panel have the same meaning as in fig. 11.

5.3 Absolute magnitude and mean colours

The well-known linear dependence of absolute magnitude vs. metallicity is shown in fig. 13. The blue line represents a linear fit of stable stars. When the slope of this dependence is considered to be the same for modulated stars, the zero-point shift with $\Delta M = 0.03$ mag appears. Very similar behaviour, based on directly observed properties of RR Lyrae variables, was noted in M5, where the difference between stable and modulated stars was found as $\Delta M_V = 0.05$ mag (Jurcsik et al. 2011). Therefore, lower luminosity can be a general property of Blazhko variables and not only due to selection bias.

To map the colour distribution of Blazhko stars among regular stars we constructed colour-magnitude (fig. 14) and colour-temperature diagrams (fig. 15). To be more conclusive, stars with different metallicity are plotted with different symbols in these plots. It is apparent that modulated stars with similar metallicity are uniformly spread out over the whole width of the dependence in fig. 14. In agreement with Arellano Ferro et al. (2012), no apparent tendency of Blazhko stars to be bluer than regular stars at any $[\text{Fe}/\text{H}]$ is seen (both groups have the average $(B-V)_0 = 0.333(2)$). On the other hand, this is contrary to the finding of Jurcsik et al.

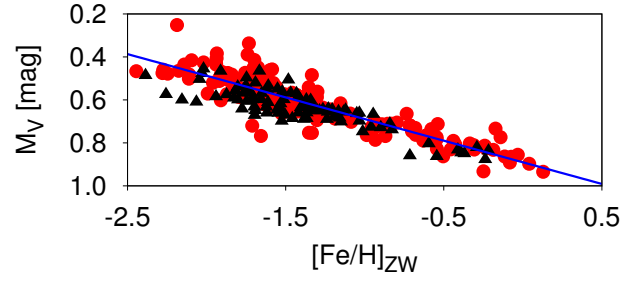


Figure 13. Metallicity dependence of absolute V-magnitude. The blue continuous line shows the LSM linear fit of regular RR Lyrae stars. Notation in the top panel is the same as in fig. 3.

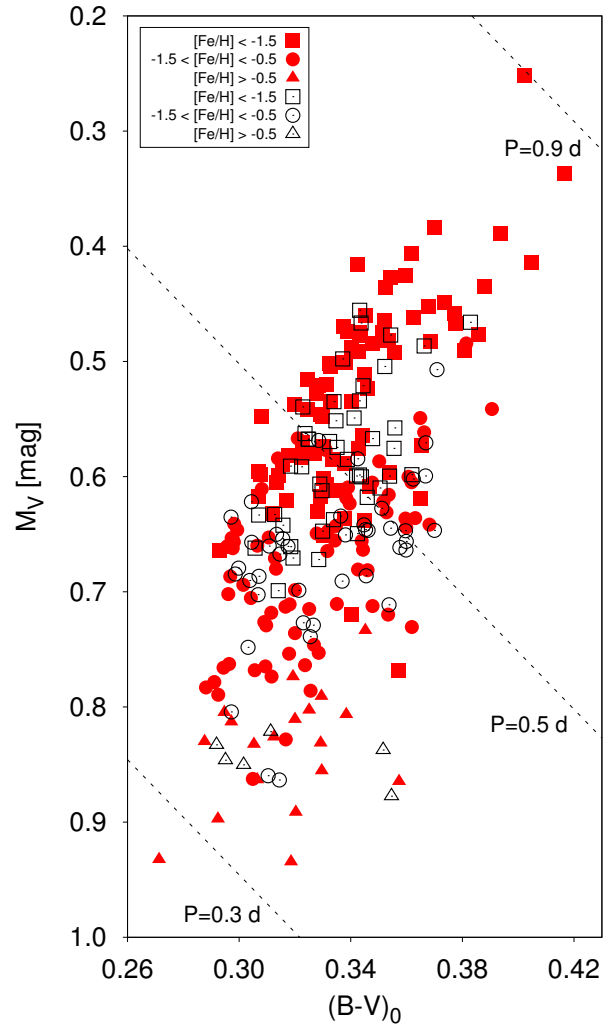


Figure 14. Colour dependence of absolute V-magnitude. Filled symbols denote RR Lyrae stars with stable light curve, while empty symbols relate to modulated stars. Dotted lines show places with constant period (labelled at each line). For more details see the text.

(2011), who proposed modulated stars in M5 to be bluer than the average. This property also needs to be investigated more closely in other stellar systems, because it seems that results on limited sample stars in M5 alone could be misleading.

For instance, lines of constant period for mean-evolved stars (equation 7 from Sandage (2010)) are plotted with dotted lines in fig. 14. When looking carefully, stars with $M_V < 0.6$ mag suggest a different dependency (different slope) than above this limit. Since metallicity correlates with absolute magnitude, as well as period, a similar linear dependence can be found for $[\text{Fe}/\text{H}]$ vs. $(B - V)_0$ and also for $[\text{Fe}/\text{H}]$ vs. period. This agrees well with figs. 1-4 of Sandage (2006).

The plot in fig. 14 is very illustrative, and many properties of RR Lyrae variables can easily be extracted from this plot. Firstly, the horizontal branch comprises horizontal layers (constant M_V) with similar metallicity. The lower the metallicity, the more luminous the star at constant $(B - V)_0$. McNamara & Barnes (2014) assigned an average absolute magnitude $M_V = 0.43$ mag to metal-poor stars from the OoII group and $M_V = 0.61$ mag to the stars from the OoI group that are more metal-rich. This corresponds well with the appearance of our fig. 14. When a star evolves blueward, its period gets shorter and vice versa. Stars with similar period, but with different colour, have different metallicity.

5.4 Short-period metal-rich variables

When effective temperature is plotted against mean $(B - V)_0$ (fig. 15), an interesting split is observed. The dependence forms two well defined sequences shifted by 180 K with continuous transition between them. From this picture it is apparent that the branches roughly follow the metal content of the stars, e.g. stars with high metallicity have higher temperature than stars with lower metallicity at a constant $(B - V)_0$. However, it is not a strict rule: a metal-strong sequence is at its blue part contaminated with a few lower-metal-abundant variables.

The upper sequence depicted in fig. 15 comprises short-period, metal-rich stars, which were mentioned in sec. 4.3 (fig. 9) to form an isolated branch in $\phi_{21}-P$ $\phi_{31}-P$ plots. These stars were marked as OoIb stars by Szczygiel et al. (2009) and were very recently discussed by McNamara & Barnes (2014), who linked them with metal-strong, short-period stars belonging to Oosterhoff group I (OoI), which are not observed in GCs. They assumed them to be Blazhko stars with $M_{\text{AveV}} = 0.89$ mag. This value corresponds very well with the appearance of fig. 14. Nevertheless, our findings clearly show that the metal-strong branch is formed mainly by stars with stable light curves, which contradicts their assumption that this sequence is populated by modulated stars. McNamara & Barnes (2014) proposed the temperature-difference between OoI and OoII stars to be 270 K, but no such split or broadening is observed in our sample.

Fig. 16 is analogous with fig. 2 of (McNamara & Barnes 2014). In this plot, OoI metal-rich stars constitute the left most sequence, while the other two branches correspond to OoI and OoII stars. The dotted lines in this plot are drawn to roughly define different Oosterhoff groups. The separation of stars into different branches in fig. 16 approximately corresponds to sequences, which are also visible in fig. 4, where the most metal-rich stars occur in the left part of the plot.

Higher temperature and lower luminosity of OoI metal-strong stars imply that they should have significantly smaller diameters than their more luminous counterparts. If the mass-metallicity dependence (eq. 8) is assumed to be continuous, a jump in periods

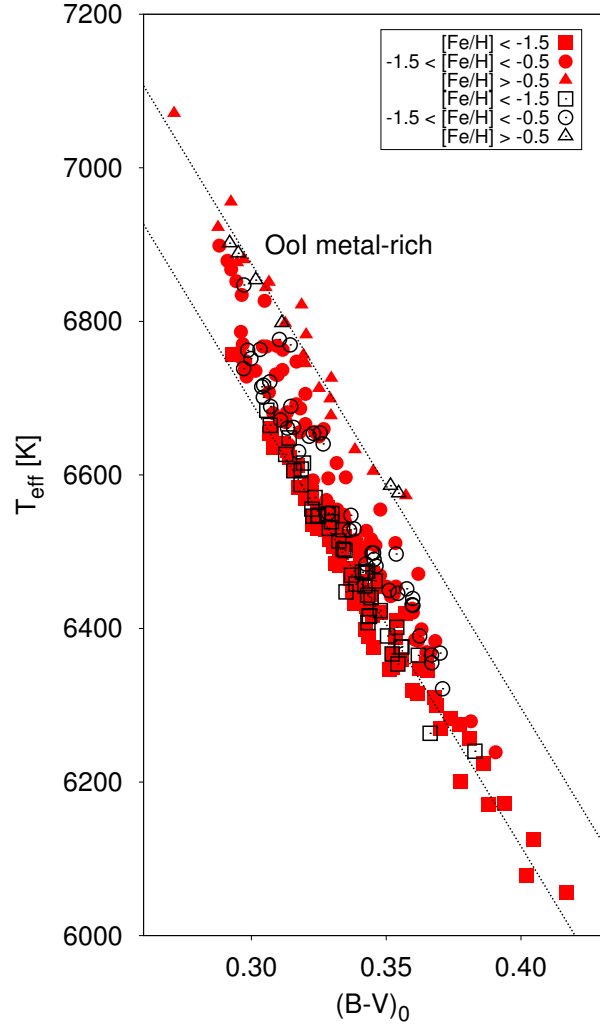


Figure 15. Effective-temperature dependence on colour index $(B - V)_0$. The bottom line represents the fit to stars with $[\text{Fe}/\text{H}]_{\text{ZW}} < -1.5$. The top line is the fit with the same slope for stars with $[\text{Fe}/\text{H}]_{\text{ZW}} > -0.5$. The zero-point difference between these two lines is 180 K. Symbols are the same as in fig. 14.

should be observed, because a lower diameter would result in a higher density which, according to pulsation equation, would lead to shorter periods. Such jump in periods is really observed in fig. 16. This new, metal-rich subclass of RR Lyrae variables is very interesting and deserves appropriate attention.

6 SUMMARY AND CONCLUSIONS

Based on data in the ASAS and WASP surveys the comparison of light-curve properties and physical characteristics of 176 RRab Lyrae stars with stable light variations, and 92 stars with the Blazhko effect was performed. Careful visual examination of each light curve was carried out. Only light curves, which were well and uniformly covered, were Fourier-decomposed. To be able to compare data from the WASP and ASAS surveys, Fourier coefficients based on WASP data were transformed to match those from ASAS through linear transformations. Since calibrations for physical pa-

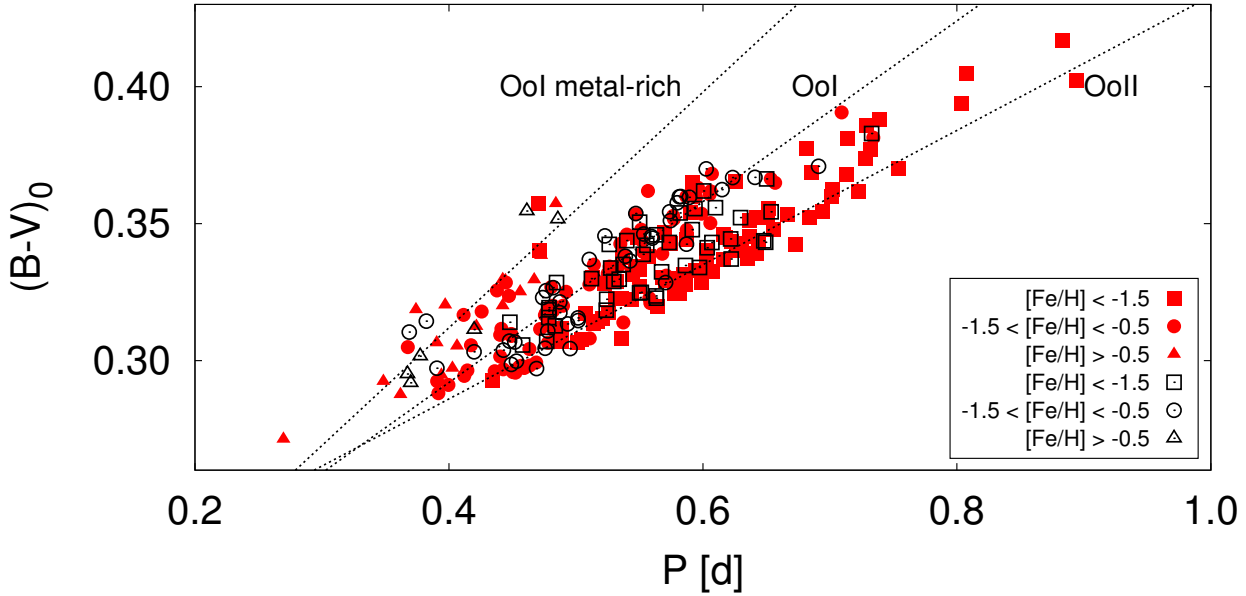


Figure 16. $(B - V)_0$ vs. P plot. Lines are only for illustration and roughly define Oosterhoff groups. For details see the text. Symbols are the same as in fig. 14.

parameters determination need Fourier parameters based on a standard V light curve, all the parameters were subsequently shifted according to K05. Based on light-curve decomposition, physical characteristics of stars were calculated using the well-known calibrations mainly from Jurcsik (1998). We assumed that these relations work for regular, as well as for modulated stars. Different parameters will than result in different physical parameters.

The main findings of this paper can be summarized in the following points:

- Blazhko stars tend to have lower total mean light change amplitudes than stars with stable light curves. This amplitude-depression is caused by higher-order amplitudes, because the average A_1 of modulated and regular stars is equivalent (see Table 4, and figures 4 and 5). A general tendency of amplitudes to get smaller with increasing period was noticed for both Blazhko and regular stars, as was expected.

- In the $\dot{\zeta}_1$ vs. R_{21} plot (fig. 6), the stars form a bent-pin dependence, where modulated stars are more or less uniformly distributed along the stem, whereas the majority of regular stars are located in the pinhead around $\dot{\zeta}_1 \approx 0.34$. Blazhko stars prefer a lower $\dot{\zeta}_1$. Below the limit of $\dot{\zeta}_1 \approx 0.3$ modulated stars constitute 69% of the whole RRab Lyrae population. In the $\dot{\zeta}_1$ vs. R_{21} diagram, long-period RR Lyrae stars prefer the stem rather than the pin-head. It was also found that more metal-deficient stars tend to be more to the left in this diagram. Nevertheless, the location of a star in this plot depends also mainly on the luminosity and mass of a star. Since the luminosity and metallicity can be determined with relatively good accuracy, it should allow theorists to precisely compute preferred masses of RR Lyrae variables.

- Dependence of ϕ_{21} and ϕ_{31} as a function of period for the LMC, SMC and GB stars is different than for field and GC stars (fig. 9) and gets steeper at $P \approx 0.55$, which is nicely seen in fig. 8. Therefore, calibrations for physical-parameters determination based on field and GC stars should not be used for LMC, SMC and GB stars, since they would probably give wrong or systemati-

cally shifted results. We guess that evolutionary effects could play a role in this observed difference.

- Blazhko stars have a longer RT compared to modulation-free stars (fig. 10). It seems that RT could be a suitable indicator of modulation, because the vast majority of regular stars have an $RT < 0.24$. Rise time of regular RR Lyrae stars plotted against other Fourier parameters follow linear dependencies, while Blazhko stars do not. This results in inconvenience of calibrations for physical parameters determination based on RT in the case of modulated stars.

- Our analysis of field RR Lyrae stars showed no convincing evidence that Blazhko stars should prefer shorter periods than other RR Lyrae variables, as in the case of modulated stars in M5 (Jurcsik et al. 2011) or in the LMC (Alcock et al. 2003). Thus, the plausibility of this assumption remains an open question.

- Blazhko stars appear at all metallicities, but may have a weak preference for lower metal content. Among stars with $[\text{Fe}/\text{H}]_{\text{ZW}} < -1$ the incidence rate of modulated stars is about 38%. Above this limit it is only about 23%. Nevertheless, the average metallicity for non-modulated stars and for Blazhko variables is equal within their uncertainties. No distinct preference of modulated stars for any of the Oosterhoff groups was found.

- Modulation-free stars are about 0.03 mag brighter than Blazhko variables, which is consistent with recent findings of Jurcsik et al. (2011) for stars in GC M5. However, the difference is very small and needs to be confirmed by further studies.

- Blazhko pulsators share the same $(B - V)_0$ as regular stars on average, which is consistent with the finding of Arellano Ferro et al. (2012) for RRab stars in M53. The discrepancy between our result and the one of Jurcsik et al. (2011) (Blazhko stars are bluer) could point out on a unique behaviour of stars in M5. However, the problem could also rise from the method - Jurcsik et al. (2011) directly measured $(B - V)$, while we determined it on the basis of semi-empirical relations using light-curve shape characteristics.

- It was found that RR Lyrae stars with the highest metal content ($[\text{Fe}/\text{H}]_{\text{ZW}} > -0.5$) are about 180 K hotter than other stars at

constant $(B - V)_0$ (fig. 15). These stars form a separate sequence in ϕ_{21} and ϕ_{31} vs. P plots (fig. 9). This group was identified recently by Szczygieł et al. (2009) and McNamara & Barnes (2014), who assigned these stars to metal-rich OoI stars with modulation. This study showed that this group comprises mainly regular RR Lyrae stars. These most metal-rich RR Lyrae variables deserve to be observed in detail to check the reliability of empirical relations for this new group of RR Lyrae pulsators.

ACKNOWLEDGMENTS

I would like to thank Miloslav Zejda, who carefully checked the text and gave interesting suggestions. I also thank my anonymous referee, who significantly helped to improve the paper. I am grateful to S. N. de Villiers for his language corrections. The WASP Consortium consists of astronomers primarily from the Universities of St Andrews, Keele, Leicester, Warwick, Queens University Belfast, The Open University, Isaac Newton Group La Palma and Instituto de Astrofísica de Canarias. WASP-North is hosted by the Isaac Newton Group on La Palma and WASP-South is hosted by SAAO. Funding for WASP comes from consortium universities and from the UK Science and Technology Facilities Council. The WASP data are stored at a server at Masaryk University Brno, Czech Republic using a new web interface, developed by the CERIT team (<http://wasp.cerit-sc.cz/form>). Work on this paper was financed by the MUNI/A/0735/2012.

REFERENCES

- Alcock, C., Alves, D. R., Becker, A., et al. 2003, *ApJ*, 598, 597
 Arellano Ferro, A., Rojas López, V., Giridhar, S., & Bramich, D. M. 2008, *MNRAS*, 384, 1444
 Arellano Ferro, A., Figuera Jaimes, R., Giridhar, S., et al. 2011, *MNRAS*, 416, 2265
 Arellano Ferro, A., Bramich, D. M., Figuera Jaimes, R., Giridhar, S., & Kuppuswamy, K. 2012, *MNRAS*, 420, 1333
 Arellano Ferro, A., Bramich, D. M., Figuera Jaimes, R., et al. 2013, *MNRAS*, 434, 1220
 Arp, H. C. 1955, *AJ*, 60, 317
 Blazhko S.N., 1907, *AN*, 175, 325
 Benkő, J. M., Kolenberg, K., Szabó, R., et al. 2010, *MNRAS*, 409, 1585
 Bryant, P. H. 2014, *ApJL*, 783, L15
 Buchler, J. R., & Kolláth, Z. 2011, *ApJ*, 731, 24
 Butters O.W. et al., 2010, *A&A*, 520, 10
 Cacciari, C., Corwin, T. M., & Carney, B. W. 2005, *AJ*, 129, 267
 Cariulo, P., Degl'Innocenti, S., & Castellani, V. 2004, *A&A*, 421, 1121
 Catelan, M., & Cortés, C. 2008, *ApJ*, 676, L135
 Catelan, M. 2009, *Ap&SS*, 320, 261
 Carretta, E., & Gratton, R. G. 1997, *A&AS*, 121, 95
 Chaboyer, B., Demarque, P., Kernan, P. J., & Krauss, L. M. 1998, *ApJ*, 494, 96
 Clement, C. M., & Shelton, I. 1997, *AJ*, 113, 1711
 Contreras, R., Catelan, M., Smith, H. A., et al. 2010, *AJ*, 140, 1766
 Deb, S., & Singh, H. P. 2014, *MNRAS*, 28
 Dékány, I., & Kovács, G. 2009, *A&A*, 507, 803
 Dziembowski, W. A., & Mizerski, T. 2004, *AcA*, 54, 363
 Gillet, D. 2013, *A&A*, 554, A46
 Goranskij, V., Clement, C. M., & Thompson, M. 2010, *Variable Stars, the Galactic halo and Galaxy Formation*, 115
 Jurcsik, J., & Kovacs, G. 1996, *A&A*, 312, 111
 Jurcsik, J. 1998, *A&A*, 333, 571
 Jurcsik, J., Clement, C., Geyer, E. H., & Domsa, I. 2001, *AJ*, 121, 951
 Jurcsik, J., Sodor, A., Varadi, M., et al. 2006, *IBVS*, 5709, 1
 Jurcsik, J., Sódor, Á., Szeidl, B., et al. 2009a, *MNRAS*, 400, 1006
 Jurcsik, J., Szeidl, B., Clement, C., Hurta, Z., & Lovas, M. 2011, *MNRAS*, 411, 1763
 Jurcsik, J., Hajdu, G., Szeidl, B., et al. 2012, *MNRAS*, 419, 2173
 Jurcsik, J., Smitola, P., Hajdu, G., et al. 2013, *ApJL*, 778, L27
 Kapakos, E., & Hatzidimitriou, D. 2012, *MNRAS*, 426, 2063
 Kinemuchi, K., Smith, H. A., Woźniak, P. R., McKay, T. A., & ROTSE Collaboration 2006, *AJ*, 132, 1202
 Kovacs, G., & Zsoldos, E. 1995, *A&A*, 293, L57
 Kovács, G., & Walker, A. R. 2001, *A&A*, 371, 579
 Kovács, G. 2005, *A&A*, 438, 227
 Kun, E., Sodor, A., Jurcsik, J., et al. 2008, *IBVS*, 5859, 1
 Layden, A. C. 1994, *AJ*, 108, 1016
 Lee, J.-W., López-Morales, M., Hong, K., et al. 2014, *ApJS*, 210, 6
 McNamara, D. H., & Barnes, J. 2014, *AJ*, 147, 31
 Mizerski, T. 2003, *AcA*, 53, 307
 Morgan, S. M., Simet, M., & Bargerquast, S. 1998, *AcA*, 48, 341
 Moskalik, P., & Poretti, E. 2003, *A&A*, 398, 213
 Nemeč, J. M. 2004, *AJ*, 127, 2185
 Nemeč, J. M., Smolec, R., Benkő, J. M., et al. 2011, *MNRAS*, 417, 1022
 Nemeč, J. M., Cohen, J. G., Ripepi, V., et al. 2013, *ApJ*, 773, 181
 Oosterhoff, P. T. 1939, *The Observatory*, 62, 104
 Oosterhoff, P. T. 1944, *BAN*, 10, 55
 Pojmanski, G. 1997, *AcA*, 47, 467
 Pojmanski, G. 2002, *AcA*, 52, 397
 Pollacco, D. L., Skillen, I., Collier Cameron, A., et al. 2006, *PASP*, 118, 1407
 Preston, G. W. 1959, *ApJ*, 130, 507
 Sandage, A. 1981, *ApJ*, 248, 161
 Sandage, A., & Cacciari, C. 1990, *ApJ*, 350, 645
 Sandage, A. 2004, *AJ*, 128, 858
 Sandage, A. 2006, *AJ*, 131, 1750
 Sandage, A. 2010, *ApJ*, 722, 79
 Shibahashi, H. 2000, *IAU Colloq. 176: The Impact of Large-Scale Surveys on Pulsating Star Research*, 203, 299
 Simon, N. R., & Lee, A. S. 1981, *ApJ*, 248, 291
 Simon, N. R., & Teays, T. J. 1982, *ApJ*, 261, 586
 Simon, N. R. 1985, *ApJ*, 299, 723
 Simon, N. R. 1988, *ApJ*, 328, 747
 Simon, N. R., & Clement, C. M. 1993, *ApJ*, 410, 526
 Skarka, M. 2014, *A&A*, 562, A90
 Smith, H. A., Catelan, M., & Kuehn, C. 2011, *RR Lyrae Stars, Metal-Poor Stars, and the Galaxy*, 17
 Smolec, R. 2005, *AcA*, 55, 59
 Smolec, R., & Moskalik, P. 2008, *AcA*, 58, 193
 Sódor, Á. 2007, *AN*, 328, 829
 Sódor, Á., Jurcsik, J., Molnár, L., et al. 2012, *Progress in Solar/Stellar Physics with Helio- and Asteroseismology*, 462, 228
 Soszyński, I., Udalski, A., Szymański, M. K., et al. 2009, *AcA*, 59, 1
 Soszyński, I., Udalski, A., Szymański, M. K., et al. 2010, *AcA*, 60, 165

- Soszyński, I., Dziembowski, W. A., Udalski, A., et al. 2011, *AcA*, 61, 1
- Szczygieł, D. M., Dziembowski, W. A., Udalski, A., et al. 2014, arXiv:1403.6476
- Stellingwerf, R. F., Nemeč, J. M., & Moskalik, P. 2013, arXiv:1310.0543
- Stothers, R. B. 2006, *ApJ*, 652, 643
- Stothers, R. B. 2010, *PASP*, 122, 536
- Szczygieł, D. M., & Fabrycky, D. C. 2007, *MNRAS*, 377, 1263
- Szczygieł, D. M., Pojmański, G., & Pilecki, B. 2009, *AcA*, 59, 137
- Szeidl, B. 1988, *Multimode Stellar Pulsations*, 45
- Udalski, A. 2003, *AcA*, 53, 291
- Udalski, A., Szymanski, M. K., Soszynski, I., & Poleski, R. 2008, *AcA*, 58, 69
- Walker, A. R., & Nemeč, J. M. 1996, *AJ*, 112, 2026
- Walker, A. R. 1998, *AJ*, 116, 220
- Wils, P., Lloyd, C., & Bernhard, K. 2006, *MNRAS*, 368, 1757
- Woźniak, P. R., Vestrand, W. T., Akerlof, C. W., et al. 2004, *AJ*, 127, 2436
- Zinn, R., West, M.J. 1984, *ApJS*, 55, 45